

Article

Comparison of the Effect of the Combination of Sodium Valproate and Sodium Dichloroacetate on the Expression of *SLC12A2*, *SLC12A5*, *CDH1*, *CDH2*, *EZH2*, and *GFAP* in Primary Female Glioblastoma Cells with That of Temozolomide

Dovydas Gečys ¹, Laimis Akramas ², Aidanas Preikšaitis ³, Ingrida Balnytė ⁴, Arūnas Vaitkevičius ⁵, Julija Šimienė ⁶  and Donatas Stakišaitis ^{4,6,*}

- ¹ Laboratory of Molecular Cardiology, Institute of Cardiology, Lithuanian University of Health Sciences, 50161 Kaunas, Lithuania; dovydas.gecys@lsmu.lt
- ² Dca Farma, UAB, 47296 Kaunas, Lithuania
- ³ Clinic of Neurology and Neurosurgery, Center of Neurosurgery, Faculty of Medicine, Vilnius University, 03101 Vilnius, Lithuania; aidanas.preiksaitis@santa.lt
- ⁴ Department of Histology and Embryology, Medical Academy, Lithuanian University of Health Sciences, 44307 Kaunas, Lithuania; ingrida.balnyte@lsmu.lt
- ⁵ Clinic of Neurology and Neurosurgery, Faculty of Medicine, Institute of Clinical Medicine, Vilnius University Hospital Santaros Klinikos, Vilnius University, 08661 Vilnius, Lithuania; arunas.vaitkevicius@santa.lt
- ⁶ Laboratory of Molecular Oncology, National Cancer Institute, 08660 Vilnius, Lithuania; julija.simiene@nvi.lt
- * Correspondence: donatas.stakisaitis@lsmu.lt

Abstract

The search for an effective treatment for adult high-grade glioblastoma (GBM) remains urgent. **Background/Objectives:** The study aimed to determine the expression of carcinogenesis-related genes, such as *SLC12A2*, *SLC12A5*, *CDH1*, *CDH2*, *EZH2*, and *GFAP*, in primary glioblastoma (WHO Grade IV; IDH-wild-type) cells from three adult women: GBM5-1, GBM5-2F, and GBM5-3F. **Methods:** The impact of the combination of sodium valproate and sodium dichloroacetate (2 mM NaVPA–3 mM NaDCA) on the expression of these genes was determined and compared with the effects of 50 µM temozolomide after 24 h of treatment. **Results:** 2 mM NaVPA–3 mM NaDCA, as well as temozolomide, had individual impacts on the *SLC12A2*, *SLC12A5*, *CDH1*, *CDH2*, *EZH2*, and *GFAP* expressions of tested GBM5-1, GBM5-2F, and GBM5-3F primary cells of female GBM patients. **Conclusions:** The combination of 2 mM NaVPA–3 mM NaDCA may have an advantage in antitumor activity and may be more effective than TMZ; however, the effect is individual.

Keywords: KCC2; NKCC1; CDH1; CDH2; EZH2; GFAP; glioblastoma; primary cells; IDH-wild-type; temozolomide; sodium valproate; sodium dichloroacetate



Academic Editor: Pedro Dorado

Received: 7 July 2025

Revised: 27 August 2025

Accepted: 2 September 2025

Published: 4 September 2025

Citation: Gečys, D.; Akramas, L.; Preikšaitis, A.; Balnytė, I.; Vaitkevičius, A.; Šimienė, J.; Stakišaitis, D.

Comparison of the Effect of the Combination of Sodium Valproate and Sodium Dichloroacetate on the Expression of *SLC12A2*, *SLC12A5*, *CDH1*, *CDH2*, *EZH2*, and *GFAP* in Primary Female Glioblastoma Cells with That of Temozolomide.

Pharmaceutics **2025**, *17*, 1161.

<https://doi.org/10.3390/pharmaceutics17091161>

Copyright: © 2025 by the authors. Licensee MDPI, Basel, Switzerland. This article is an open access article distributed under the terms and conditions of the Creative Commons Attribution (CC BY) license (<https://creativecommons.org/licenses/by/4.0/>).

1. Introduction

Adult diffuse glioblastoma (GBM) is the most aggressive brain tumor type with the worst prognosis; high-grade glioblastoma has a 5-year overall survival (OS) of 5% of patients [1]. GBMs (WHO Grade IV) are classified as primary brain tumors, as IDH-wild-type GBMs, which represent the most frequent malignant brain tumors, with an OS ranging from 12 to 18 months [2]. Women are slightly less likely to suffer from GBM and have a slightly better median survival than men [3]. GBM is a highly heterogeneous tumor in which different cell types coexist, including tumor cells, fibroblasts, endothelial cells, and immune cells [4–6]. GBM subtypes can coexist in different tumor parts and within their

cells [7]. Differences in tumor tissue are found between different stages, genders, and age groups. High heterogeneity of tumor cells is associated with invasive and metastatic manifestations [8].

The approach to GBM treatment to date is to personalize each clinical case, considering the diagnosis time, onset or relapse, age, tumor cancer markers, and the patient's general condition. The current standard treatment approach for newly diagnosed GBM involves tumor-maximal surgical resection with radiotherapy and temozolomide (TMZ) therapy [9]. Chemotherapy is a key part of the treatment regimen for adult patients [10]. TMZ was registered in 2005 for the treatment of newly diagnosed GBM [11,12]. Treatment of GBM after surgery with the addition of TMZ to radiotherapy has increased OS by 2 months [13], with a median OS of 15 months and progression-free survival of 6 months. In more than 50% of patients with GBM, TMZ treatment is ineffective [14,15]. TMZ is only helpful in patients with GBM with a methylated-DNA-protein-cysteine methyltransferase (MGMT) promoter, which is slightly more common in women than in men, supporting their better survival outcomes, but the toxic effects of chemotherapeutic agents are more common in women [16]. Thus, there is currently no effective treatment for GBM, and the search for one, especially for individualized treatment with higher efficacy and lower toxicity, is urgent.

The primary effects of drugs on GBM are related to the inhibition of tumor cell proliferation and the activation of apoptosis [17]. Activated glycolytic processes characterize GBM cells [18]. Tumor cells exhibit increased expression of pyruvate dehydrogenase kinases (PDKs), leading to enhanced glycolytic activity in GBM cells [19,20]. Consequently, inhibition of PDKs is a target for GBM treatment [21].

As an anticancer preparation, sodium dichloroacetate (NaDCA) selectively acts on cancer cells by inhibiting PDK [22], thereby activating pyruvate dehydrogenases (PDHs), which reduces lactate levels in both the blood and the tumor microenvironment, inhibiting tumor growth and spread [23]. Preclinical studies have shown that NaDCA salts are associated with a reduction in tumor cell proliferation rate and metastatic spread, and activation of apoptosis [22]; NaDCA inhibits U87 MG and PBT24 glioblastoma xenografts growth, frequency of tumor invasion, and the number of blood vessels in the chicken chorioallantoic membrane model; NaDCA impacts on tumor proliferating cell nuclear antigen (PCNA) and enhancer of zest homolog 2 (EZH2) expression in the tumor tissue cells [24]. Studies of immunodeficient mice with U87 tumors in the brain have shown that the combination of NaDCA and radiotherapy increases the survival of the mice [25].

Sodium valproate (NaVPA) is a histone deacetylase (HDAC) inhibitor, specifically targeting classes I and IIa, and an epigenetic modulator that affects gene expression by inhibiting tumor cell proliferation and inducing apoptosis [26,27]. HDACs may regulate GBM progression. HDAC2 expression is upregulated in GBM cells. Knockdown of HDAC2 inhibits GBM cell proliferation and invasion, suggesting that HDAC2 may be a potential target for treating GBM and enhancing the efficacy of TMZ therapy [28]. HDAC2 knockdown inhibits glioblastoma tumorigenesis through regulating glucose metabolism and proliferation [29]. NaVPA alone or combined with other therapies inhibits glioma growth in vivo and in vitro [30]. Non-toxic doses of NaVPA increase the sensitivity of U87 and T98G cells to gefitinib by inhibiting cell growth through the activation of autophagy [31]. NaVPA binds E2F transcription factor 1 to the glycosylated GPI and PGK1 promoter to inhibit glycolysis [32]. NaVPA may enhance the transport of the dichloroacetate anion into the cell via mitochondrial mechanisms [33,34]. The synergistic effects of chemotherapy and HDAC inhibitors are promising for treating GBM and preventing chemotherapy resistance [35].

The inflammatory microenvironment of the GBM tumor, characterized by the release of pro-inflammatory cytokines and chemokines, as well as the activation of inflammatory

pathways, promotes tumor malignancy, which is associated with increased resistance of GBM to therapy [36,37]. Changes in the microenvironment of cancer tissues are characterized by increased lactic acid content [38]. NaDCA is an investigational antitumor drug with anti-inflammatory properties [39]. NaVPA's immunomodulatory and anti-inflammatory effects are also well-established [40,41]. Treatment with NaVPA–NaDCA increased *Slc5a8* expression in mouse thymocytes, indicating an effect of NaVPA on the dichloroacetate anion transporter, and significantly affected the expression of genes related to inflammation and immune response [42]. Experimental research data, both in vivo and in vitro, indicate that NaVPA–NaDCA exhibits a more effective anticancer effect on GBM compared to NaDCA, and its efficacy surpasses that of TMZ. However, the effects of the investigational drugs on GBM differ depending on the cell line [43]. NaVPA–NaDCA inhibits inflammatory and immune response pathways [44], which are also characteristic of GBM.

Understanding the mechanisms of action of drugs and the evolution of resistance to treatment is crucial for the efficacy of GBM treatment, as it enables the assessment of the impact of drugs on changes in cancer prognostic markers [45,46]. Advances in the personalized treatment of GBM are closely tied to standard treatment, and new treatment strategies are being explored, including chemotherapy with drugs targeting the molecular and metabolic properties of the tumor [47,48]. Tumor cell proliferation and epithelial–mesenchymal transition (EMT) are central regulators of GBM invasion and are regulated by several factors that determine and promote cancer progression, related to the glycolytic phenotype of cells, which is closely linked to GBM malignancy [49]. The Na–K–2Cl cotransporter (NKCC1, encoded by *SLC12A2*) increases intracellular Cl^- concentration and enhances GBM cell proliferation [50–52], and it is involved in the EMT process. The K–Cl cotransporter (KCC2; encoded by *SLC12A5*) regulates the efflux of K^+ and Cl^- ions from the cell. Apoptosis requires a loss of cell volume, which occurs through the reduction in intracellular $[\text{K}^+]_i$ and $[\text{Cl}^-]_i$, before any other detectable features of apoptosis are observed. Loss of $[\text{K}^+]_i$ and $[\text{Cl}^-]_i$ in the glioma cell in parallel with expressed apoptosis was confirmed [53–55]. A EMT in part is a result of the downregulation of E-cadherin (*CDH1*) and the parallel upregulation of N-cadherin (*CDH2*) genes [56]. Downregulation of *CDH1* might be related to the induction of EMT [57]. It was reported that by regulating *SLC12A5* expression, EZH2 activates the WNK1–OSR1–NKCC1 (lysine-deficient protein kinase-1—oxidative stress responsive 1—NKCC1) pathway to promote glioma migration and tumor invasion, while also promoting *SLC12A5* DNA methylation [58]. EZH2's role in regulating *GFAP* (glial fibrillary acidic protein) expression may offer insights into the molecular mechanisms of GBM [59,60]. Understanding this interplay could elucidate the pathophysiology of *GFAP* expression and help develop strategies for targeting GBM progression [60]; therefore, the exact mechanism in GBM needs further exploration.

The study aimed to determine the differences in the primary cell response of IDH-wildtype GBMs to treatment with the sodium valproate and sodium dichloroacetate combination (NaVPA–NaDCA) by assessing the expression of cancer marker genes *SLC12A2*, *SLC12A5*, *CDH1*, *CDH2*, *EZH2*, and *GFAP*, and to compare these effects with those of TMZ.

NaVPA–NaDCA and TMZ had individual effects on the expression of *SLC12A2*, *SLC12A5*, *CDH1*, *CDH2*, *EZH2*, and *GFAP* in GBM5-1, GBM5-2F, and GBM5-3F primary cells. The study suggests that the NaVPA–NaDCA combination may have an anticancer activity advantage over TMZ, but the effect depends on the patient's cells. It is essential to assess the sensitivity of GBM cells to the drug before initiating chemotherapy when determining a treatment strategy.

2. Materials and Methods

2.1. GBM Patient Clinical Data

The inclusion criteria for study patients were as follows: adult patients with a first diagnosis of GBM, who had not received anticancer drugs and were not using valproic acid. GBM tissue samples were obtained from three patients who underwent surgery, and their details are provided below. GBM5-1F, 45-year-old female; glioblastoma diffuse (WHO Grade IV), IDH-wild-type; tumor of the left-sided frontoparietal region with spread to the basal ganglia and upper part of the brain stem; strong positive cytoplasmic reaction in GFAP tumor cells (surgery 28 November 2024); GBM5-2F, 77-year-old female; GBM diffuse (WHO Grade IV), IDH-wild-type; left frontal region tumor; strong positive cytoplasmic reaction in GFAP tumor cells (surgery 6 January 2025); GBM5-3F, 83-year-old female; GBM diffuse (WHO Grade IV), IDH-wild-type; tumor of the left parietoccipital area; strong positive cytoplasmic reaction in GFAP tumor cells (surgery 24 March 2025). The Vilnius Regional Biomedical Research Ethics Committee granted authorization to conduct biomedical research on 11 November 2024, under authorization No. 2024/11-1625-1077. Patients were operated on at Vilnius University Santaros Hospital Neurosurgery Clinic (Santariškių St. 2, Vilnius); patients were not treated with anticancer drugs prior to surgery.

2.2. Preparation of Cells for Analysis from Tumor Tissue

The explanted tumor tissue was placed in Ca^{2+} -depleted Dulbecco's Modified Eagle Medium (ThermoFisher Scientific, Gibco, Rotterdam, The Netherlands) supplemented with 1% penicillin-streptomycin (ThermoFisher Scientific, Gibco, Rotterdam, The Netherlands); the time taken to harvest the tumor for analysis after tumor removal was no longer than 10 min, and the tissue was kept at 37 °C in the medium. In a Ca^{2+} -free medium, the tissue was dissected into small pieces using needle tweezers and then gently pipetted to obtain a cell suspension. Suspension was centrifuged at $110\times g$ for 5 min, and the supernatant was discarded. Cells were seeded into 6-well multiwell tissue culture plates (TPP, Trasadingen, Switzerland) and grown in depleted Dulbecco's Modified Eagle Medium (ThermoFisher Scientific, Gibco, Rotterdam, The Netherlands) supplemented with 10% fetal bovine serum (ThermoFisher Scientific, Gibco, Rotterdam, The Netherlands) and 1% penicillin-streptomycin (ThermoFisher Scientific, Gibco, Rotterdam, The Netherlands) under standard conditions at 37 °C and 5% CO_2 . Experimental groups comprised control, NaVPA–NaDCA, and TMZ groups, in which cells were treated with a phosphate-buffered saline (ThermoFisher Scientific, Gibco, The Netherlands), 2 mM NaVPA, and 3 mM NaDCA (Sigma Aldrich, Steinheim, Germany) combination or 50 μM TMZ (Sigma Aldrich, Steinheim, Germany), respectively, for 24 h. After incubation, cells were scraped, transferred into a sterile 15 mL tube, and centrifuged at $110\times g$ for 5 min. The supernatant was discarded, and fresh cell pellets were used to extract the RNA.

2.3. Total RNA Extraction and Real-Time qPCR

Total RNA was extracted from the cells using the TRIzol™ Plus RNA Purification Kit (Invitrogen™, Thermo Fisher Scientific, Rotterdam, The Netherlands). The concentration of the extracted RNA was measured with a NanoDrop 2000 spectrophotometer (Thermo Scientific, Waltham, MA, USA). RNA was reverse transcribed into cDNA using the High-Capacity cDNA Reverse Transcription Kit (Applied Biosystems™, Thermo Fisher Scientific, Rotterdam, The Netherlands), with the addition of RNaseOUT™ Recombinant Ribonuclease Inhibitor (Invitrogen™, Thermo Fisher Scientific, Rotterdam, The Netherlands). Real-time PCR for *SLC12A2* (TaqMan Assay ID: Hs00169032_m1), *SLC12A5* (TaqMan Assay ID: Hs00221168_m1), *CDH1* (TaqMan Assay ID: Hs01023895_m1), *CDH2* (TaqMan Assay ID: Hs00983056_m1), *EZH2* (TaqMan Assay ID: Hs00544830_m1) and *GFAP* (TaqMan Assay ID:

Hs00909233_m1) were carried out using TaqMan chemistry (Applied Biosystems™, Thermo Fisher Scientific, Rotterdam, The Netherlands) following the manufacturer's protocol on a 7900 Real-Time PCR System (Applied Biosystems™, Thermo Scientific, Carlsbad, CA, USA). All reactions were performed in triplicate. The glyceraldehyde-3-phosphate dehydrogenase gene (*GAPDH*) was used as the reference gene (TaqMan Assay ID: Hs02786624_g1).

2.4. Investigational Medicinal Preparations

Investigational medicinal preparations used for the study were sodium valproate (NaVPA; Sigma-Aldrich, Steinheim, Germany), sodium dichloroacetate (NaDCA; Sigma-Aldrich, Steinheim, Germany), and temozolomide (Sigma-Aldrich, St. Louis, MO, USA). The combination of NaVPA and NaDCA is patented: a patent filed that covers VPA–NaDCA as a new medicinal product for the treatment of cancer (Official bulletin of the State Patent Bureau of the Republic of Lithuania, No. 6874, filing date 17 April 2020); a European patent application has been submitted (European patent application No. 21168796.7, filing date 16 April 2021). Primary GBM cells were treated with 2 mM NaVPA and 3 mM NaDCA combination (NaVPA–NaDCA) for 24 h. The doses of the investigational drugs were selected based on studies conducted in vivo and in vitro with GBM cell lines [43]. The selected TMZ concentration for cell treatment corresponds to the average blood plasma concentration in patients treated with TMZ [61].

2.5. Statistical Analysis

Statistical analysis and graphs were generated using GraphPad Prism 9 software (GraphPad Software, Inc., San Diego, CA, USA). For statistical purposes, the threshold cycle (CT) values of single PCR replicates were normalized to the control *GAPDH* for gene expression analysis, and the Δ CT value was calculated, which was further used for statistical tests. The Shapiro–Wilk test was used to verify the normality assumption. Most of the samples had a Gaussian distribution; however, due to the small sample size within groups, non-parametric tests were used. The difference between the two independent groups was evaluated using the Mann–Whitney *U* test. Kruskal–Wallis test with Benjamini, Krieger, and Yekutieli multiple comparisons correction was used to determine differences between the medians of three independent groups (Tables S1–S6). The Livak ($2^{-\Delta\Delta CT}$) method was used to calculate the expression between the treated and control groups of the investigated genes. The alterations in gene expression are presented as percentages and were calculated from fold change values, assuming that a fold change of 2 represents a 100% increase and a fold change of 0.5 corresponds to a 50% decrease in gene expression. Statistical significance was defined as $p < 0.05$.

3. Results

The data from the gene expression assays are tabulated in the Supplementary Materials: Tables of Supplementary Data (Tables S1–S6), which presents the tested gene expressions in control cells and the gene expression after treatment with the test drugs compared to the control.

3.1. The Effect of NaVPA–NaDCA or TMZ on the *SLC12A2* Expression in Female GBM Patients' Tumor Primary Cells

Figure 1 presents the *SLC12A2* expression data of the tested primary GBM cells (control and treated with NaVPA–NaDCA or TMZ) from women who underwent surgery.

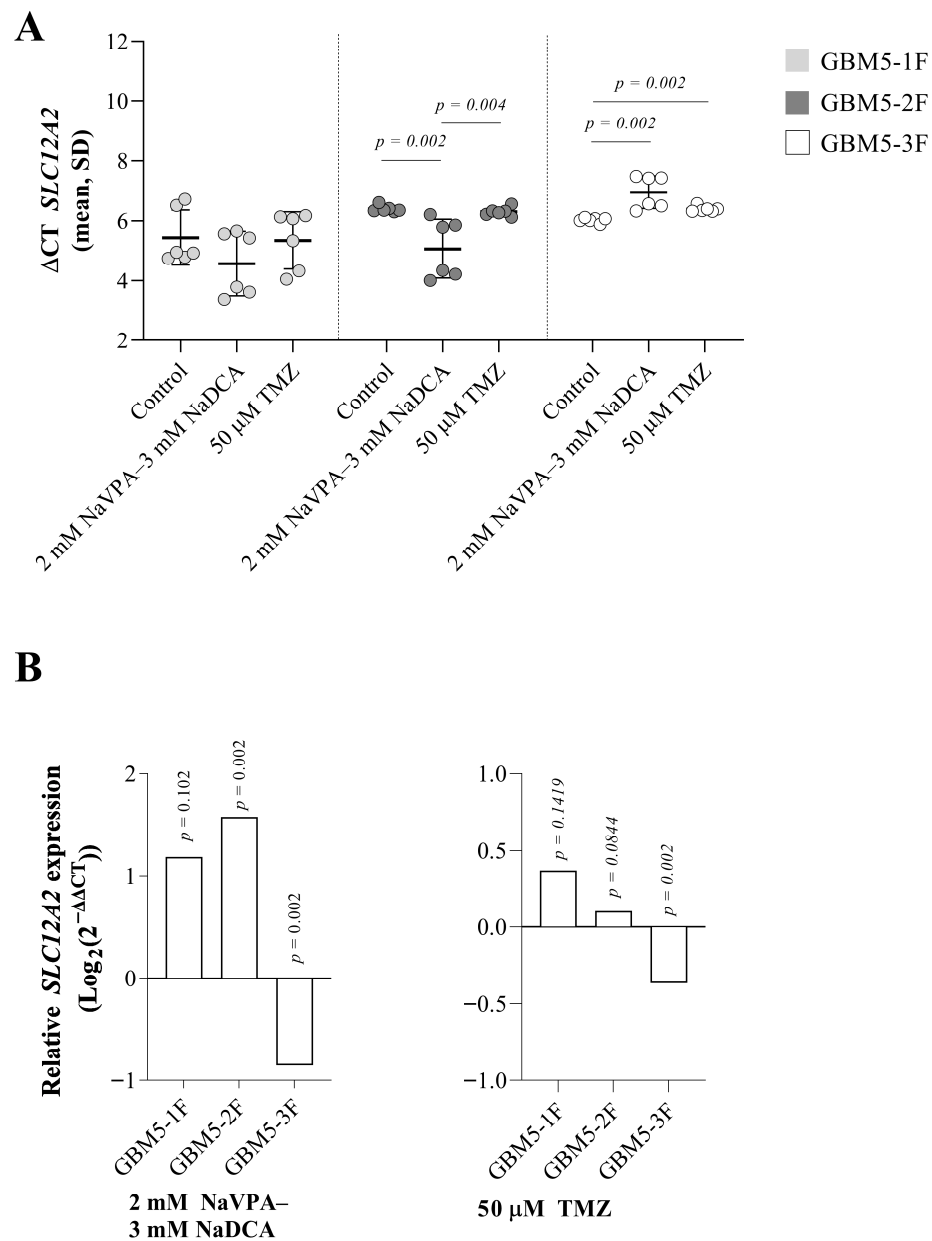


Figure 1. (A) The *SLC12A2* expression (ΔCT) of the GBM patient tumor control group, normalized to the *GAPDH*. (B) Relative *SLC12A2* expression ($\text{Log}_2(2^{-\Delta\Delta\text{CT}})$) of female GBM patient tumor groups tested. Exact *p*-values are given compared to the control.

There was no difference in *SLC12A2* expression in GBM-1F control cells compared to GBM5-2F control and GBM5-3F control cells, but when comparing the latter two, GBM5-2F cells had significantly lower gene expression than GBM5-3F cells ($p = 0.002$). Figure 1B depicts significant relative *SLC12A2* expression differences between GBM5-2F- and GBM5-3F-treated and their control groups.

Treatment with 2 mM NaVPA-3 mM NaDCA significantly increased the expression of *SLC12A2* in GBM5-1F and GBM5-2F cells (130% and 200%, respectively), but upregulation of *SLC12A2* was not significantly different between GBM5-1F and GBM5-2F tumor cells after treatment with NaVPA-NaDCA. Combination treatment significantly reduced gene expression by 45% in GBM5-3F cells compared to the control. TMZ reduced *SLC12A2* expression in GBM5-3F cells by 22% compared to the control, but did not affect *SLC12A2* expression in other patient cells treated with TMZ (Figure 1B).

3.2. The Effect of NaVPA–NaDCA or TMZ on the *SLC12A5* Expression in Female GBM Patients' Tumor Primary Cells

The expression of *SLC12A5* was significantly different in all control cells tested ($p = 0.002$). Specifically, GBM5-3F cells exhibited the highest gene expression ($p = 0.002$), while GBM5-1F cells had significantly lower expression than GBM5-3F cells ($p = 0.009$).

Figure 2A demonstrates that *SLC12A5* expression increased in GBM5-1F and GBM5-2F cells but decreased in GBM5-3F cells after NaVPA–NaDCA treatment. TMZ had no impact on gene expression. All cells treated with the combination showed higher *SLC12A5* expression than those treated with TMZ.

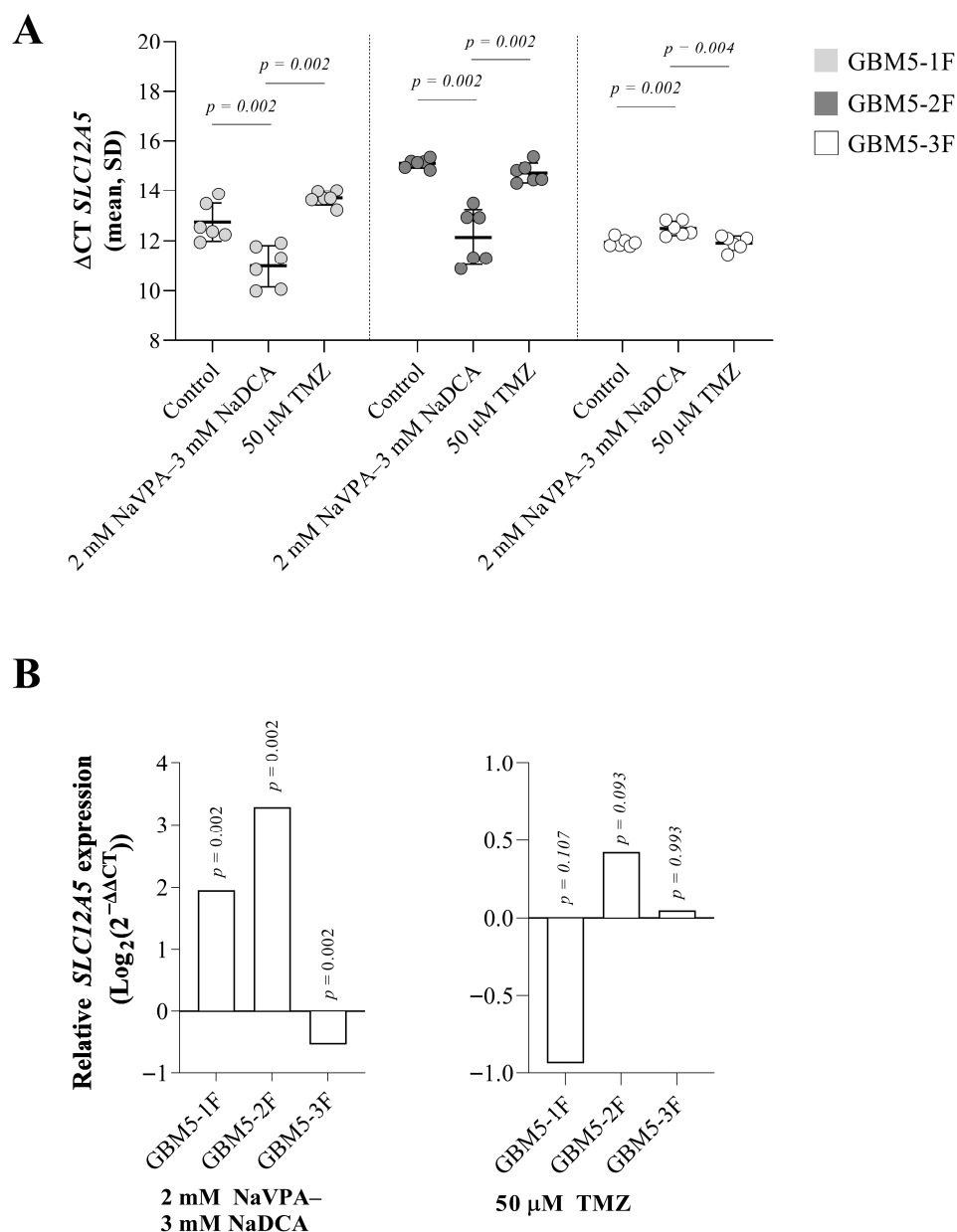


Figure 2. (A) The *SLC12A5* expression (ΔCT) of the GBM patient tumor control group was normalized to the *GAPDH*. (B) Relative *SLC12A5* expression ($\text{Log}_2(2^{-\Delta\Delta\text{CT}})$) of female GBM patient tumor groups tested. Exact p -values are given compared to the control.

Compared to the control, NaVPA–NaDCA treatment significantly increased relative *SLC12A5* expression in GBM5-1F and GBM5-2F (by 387% and 870%, respectively). The upregulation of *SLC12A5* was not significantly different between GBM5-1F and GBM5-2F

tumor cells after treatment ($p > 0.05$). In contrast, treatment with 2 mM NaVPA—3 mM NaDCA significantly reduced relative gene expression by 31% in GBM5-3F cells compared to its control. TMZ treatment did not affect *SLC12A5* expression in all three cells tested.

3.3. The Effect of NaVPA–NaDCA or TMZ on the *CDH1* Expression in Female GBM Patients' Tumor Primary Cells

CDH1 expression was detected in all control cells, with the highest expression levels observed in GBM-2F and GBM-3F, showing no significant difference between them. These cells exhibited significantly higher expression compared to GBM-1F cells ($p = 0.002$).

The combination treatment significantly increased *CDH1* expression in GBM5-1F by 123%, while no significant changes in gene expression were detected in the other two patient cells. Upregulation of *CDH1* was significantly different ($p = 0.0051$) between GBM5-1F and GBM5-2F cells after treatment with NaVPA–NaDCA. TMZ only reduced *CDH1* expression by 29% in GBM5-1F cells (Figure 3B).

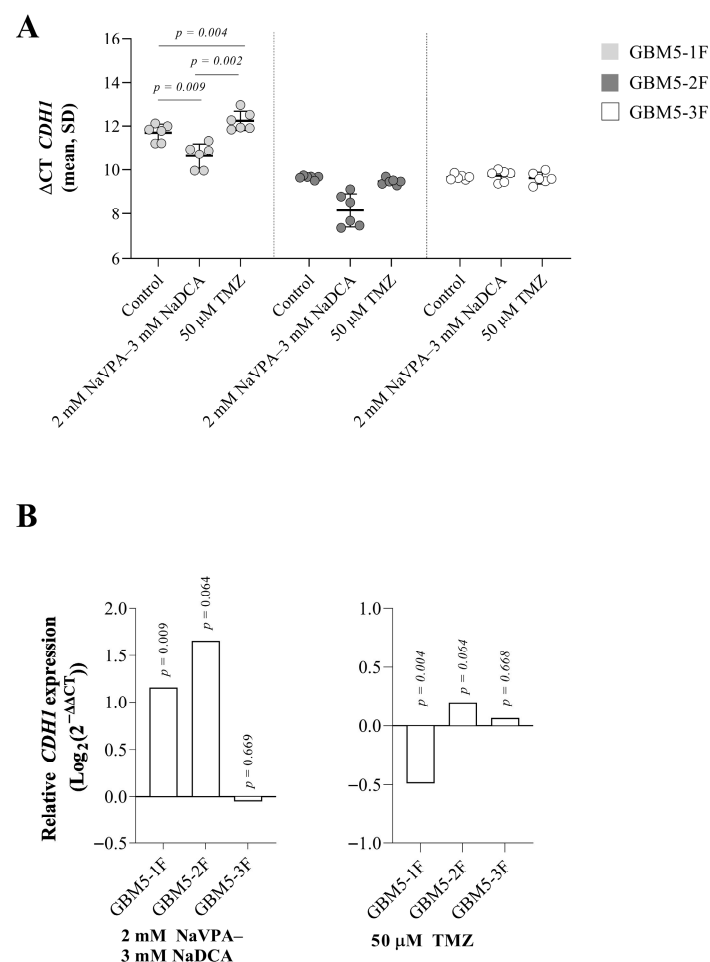


Figure 3. (A) The *CDH1* expression (ΔCT) of the GBM patient tumor control group, normalized to the *GAPDH*. (B) Relative *CDH1* expression ($\text{Log}_2(2^{-\Delta\Delta CT})$) of female GBM patient tumor cell treated groups. Exact p -values are given compared to the control.

3.4. The Effect of NaVPA–NaDCA or TMZ on the *CDH2* Expression in Female GBM Patients' Tumor Primary Cells

The controls of GBM5-1F and GBM5-2F had similar *CDH2* expression, and their gene expression was significantly higher than that of GBM5-3F cells ($p = 0.05$). NaVPA–NaDCA treatment had no significant effect on *CDH2* expression in all three patients' cells studied, but TMZ treatment significantly reduced relative gene expression in GBM5-1F and GBM5-

2F cells (14% and 6%, respectively) and did not affect gene expression in GBM5-3F cells compared to the control (Figure 4B).

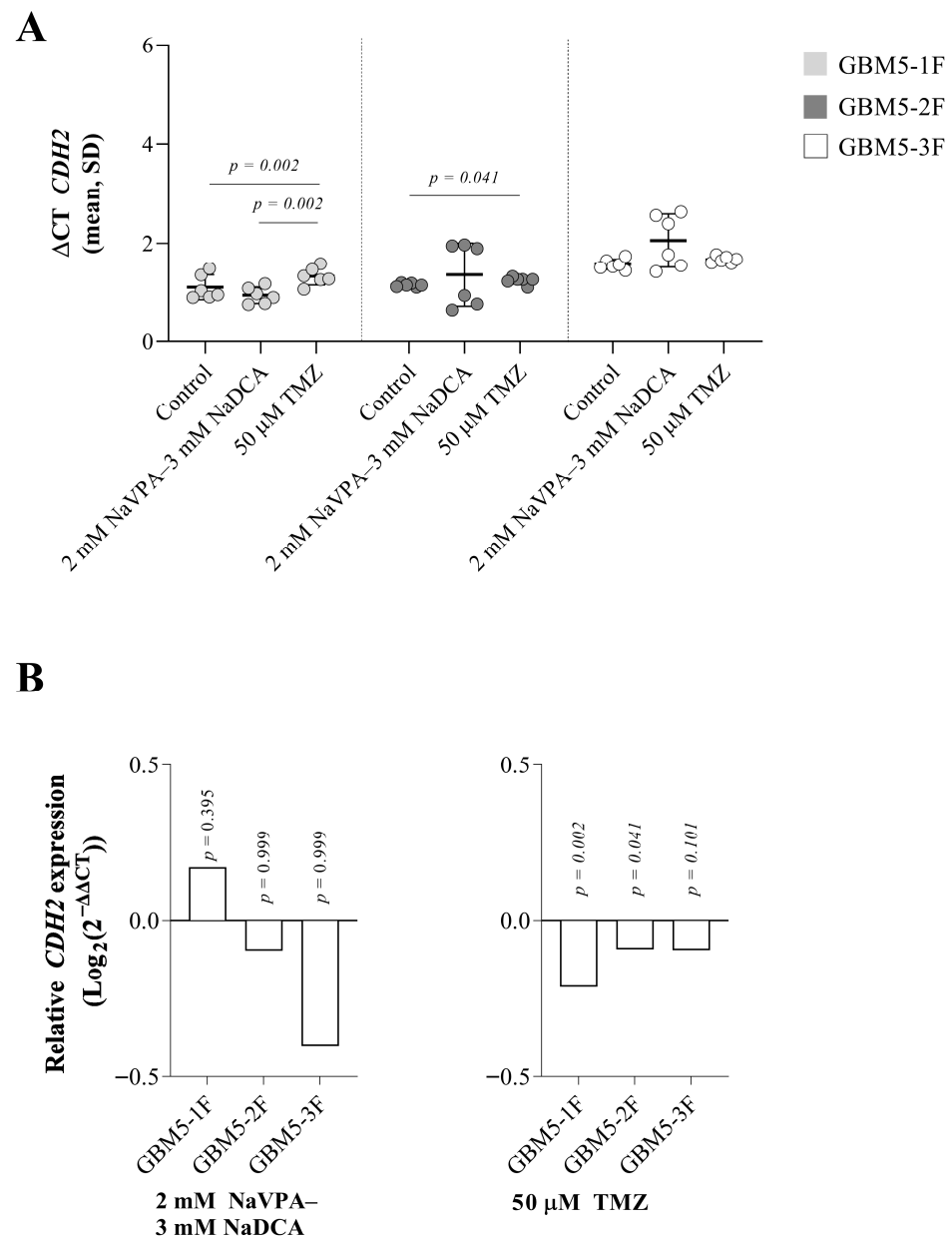


Figure 4. (A) *CDH2* expression (ΔCT) of GBM patient tumor control cell groups normalized to the *GAPDH* gene. (B) Relative *CDH2* expression ($\text{Log}_2(2^{-\Delta\Delta\text{CT}})$) of female GBM patient tumor groups tested. Exact p-values are given compared to the control.

3.5. The Effect of NaVPA–NaDCA or TMZ on the *EZH2* Expression in Female GBM Patients' Tumor Primary Cells

There were differences in *EZH2* expression between the control cells tested. Comparing GBM-1F and GBM-2F cells, no difference in gene expression was found; however, GBM5-1F cells exhibit significantly lower gene expression than GBM5-3F cells ($p = 0.002$). GBM5-2F cells exhibit significantly lower *EZH2* expression compared to GBM5-3F cells.

Treatment with 2 mM NaVPA–3 mM DCA significantly increased relative *EZH2* expression in GBM5-1F cells by 168% and in GBM5-2F by 163%. (upregulation of *EZH2* was not significantly different between GBM5-1F and GBM5-2F cells after treatment with NaVPA–NaDCA), and significantly reduced GBM5-3F gene expression by 28% compared

to the controls. TMZ significantly increased gene expression by 6% in GBM5-2F cells only (Figure 5B). After NaVPA–NaDCA treatment, *EZH2* expression was significantly higher in GBM5-1F and GBM5-2F and lower in GBM5-3F compared to the corresponding groups treated with TMZ.

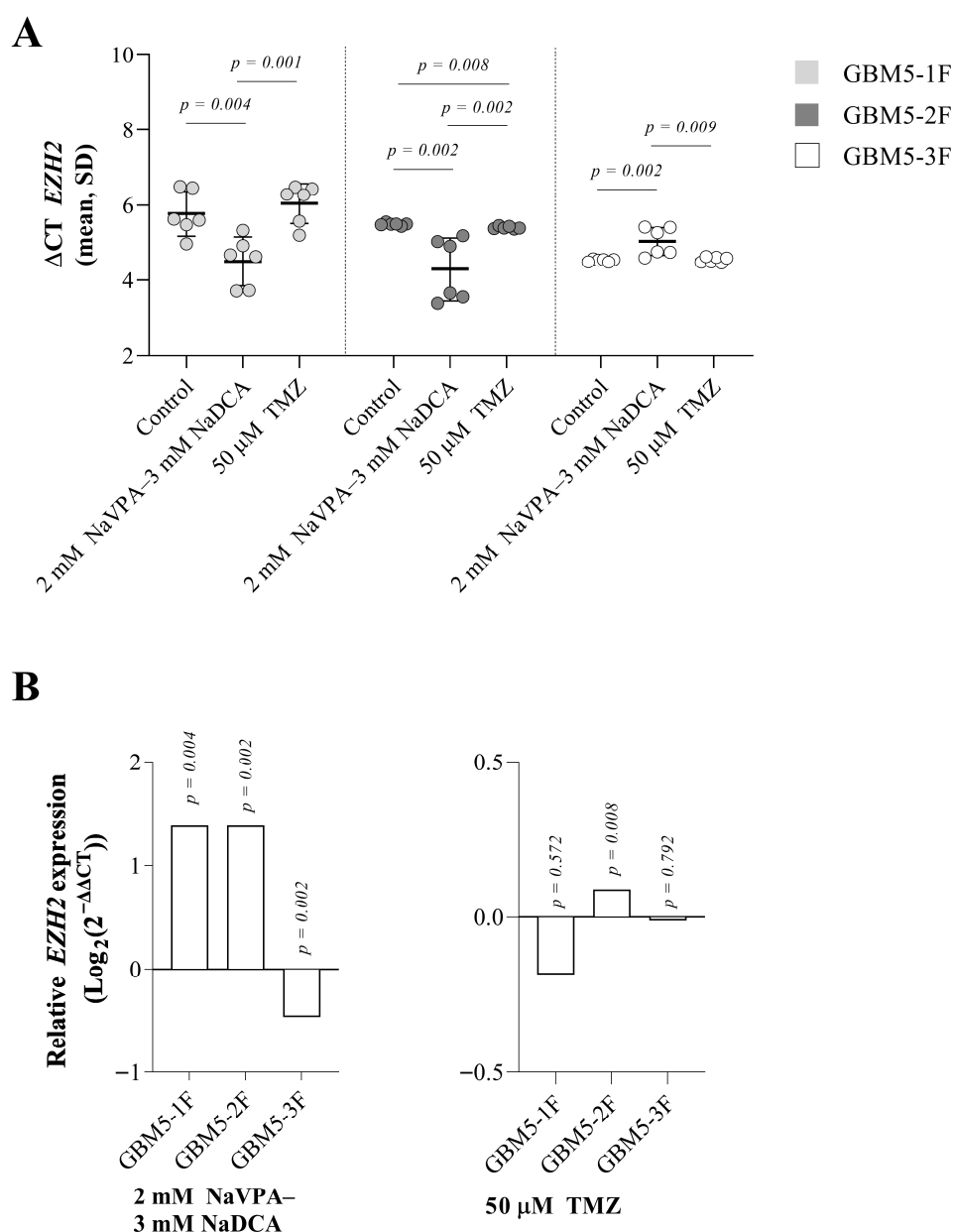


Figure 5. (A) The *EZH2* expression (ΔCT) of the GBM patient tumor control group was normalized to the *GAPDH*. (B) Relative *EZH2* expression ($\text{Log}_2(2^{-\Delta\Delta\text{CT}})$) in female GBM patient tumor cell treated groups. Exact *p*-values are given compared to the control.

3.6. The Effect of NaVPA–NaDCA or TMZ on the GFAP Expression in Female GBM Patients' Tumor Primary Cells

The following differences in *GFAP* expression were observed between the control and test cells: gene expression was significantly lower in GBM5-2F compared to GBM5-1F ($p = 0.002$); the gene expression in GBM5-3F cells was significantly higher than in GBM5-2F ($p = 0.002$).

Treatment with 2 mM NaVPA–3 mM NaDCA significantly upregulated *GFAP* expression by 224% in GBM5-2F and significantly downregulated gene expression by 35%

in GBM5-3F cells compared with control levels and did not affect gene expression in GBM5-1F cells. TMZ treatment did not affect *GFAP* expression compared with control levels (Figure 6A,B).

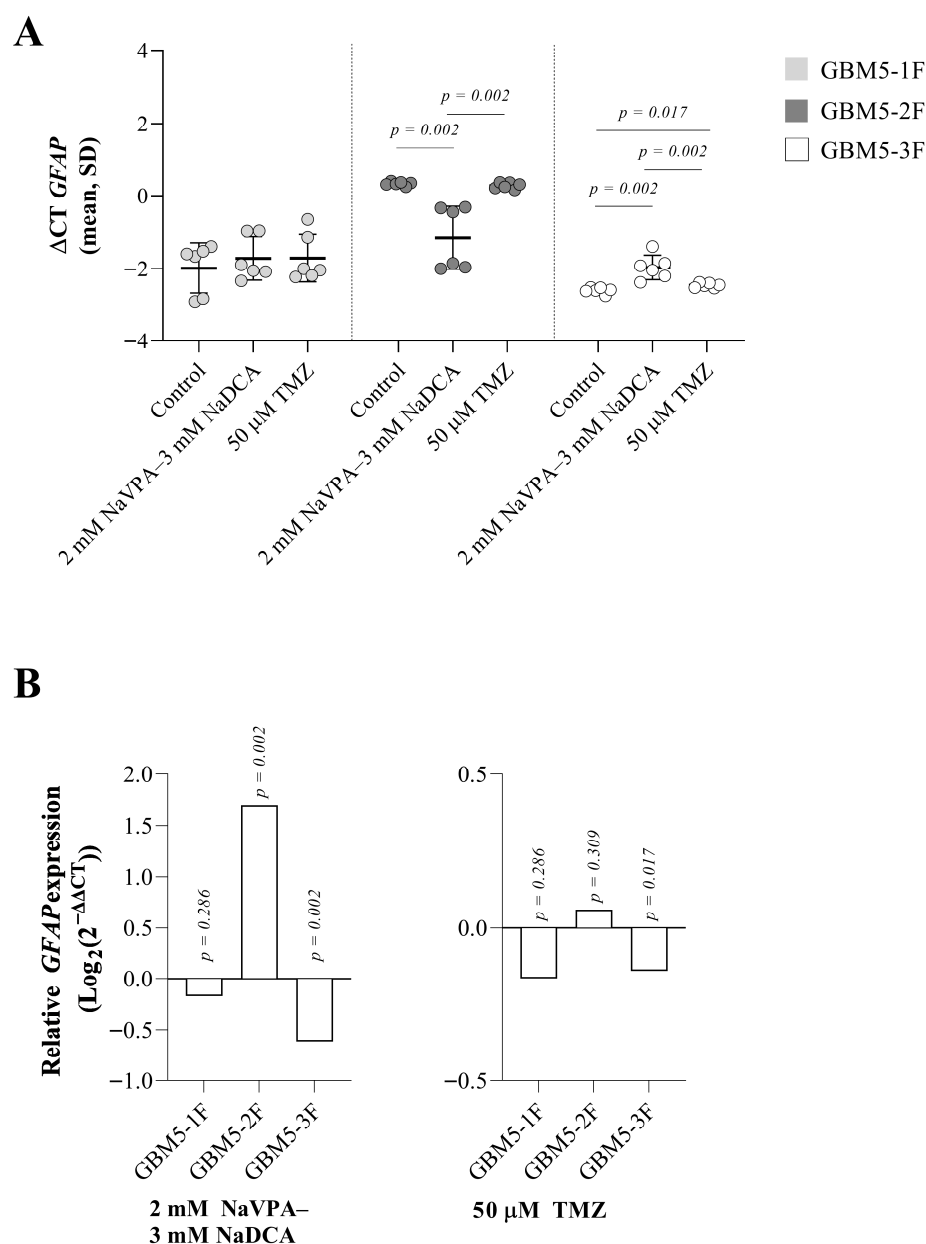


Figure 6. (A) The *GFAP* expression (ΔCT) of the GBM patient tumor control group was normalized to the *GAPDH* gene. (B) Relative *GFAP* expression ($\text{Log}_2(2^{-\Delta\Delta\text{CT}})$) of female GBM patient tumor treated cell groups. Exact p -values are given compared to the control.

4. Discussion

Glioblastoma (GBM) is a very aggressive type of glioma that practically recurs after first-line standard treatment with surgery, radiotherapy, and TMZ chemotherapy [62]. Five-year survivors of IDH-wild-type GBM patients represent a minority of the GBM population, and the differences in their molecular mechanisms compared to patients whose treatment was ineffective remain largely unexplored [63]. The invasive nature of GBM tumors is linked to the intercellular communication system used by cells to adapt to the microenvironment [64]. Characterizing the heterogeneity and invasiveness of patients'

tumors is challenging for research, and so is identifying targeted, personalized treatment approaches [7,65].

Experimental studies with GBM cell lines have shown that NaVPA–NaDCA exhibits anticancer effects on GBM by inhibiting tumor growth, invasion, proliferation, and angiogenesis, and its efficacy may be superior to that of TMZ. However, the efficacy of the investigational medicines depends on the GBM cell lines [43]. Macrophages, monocytes, and microglia cells are essential for GBM growth, and invasion is inhibited when these inflammatory and immune cells are suppressed [66]. However, the exact pathways involved in the tumor-sustaining process have not been characterized. Experimental and biomedical studies on T lymphocytes have shown that NaVPA–NaDCA inhibits inflammatory and immune pathways necessary for the growth of GBM; gene sequence analysis revealed a significant effect of NaVPA–NaDCA on inhibiting inflammatory mechanisms, leading to the downregulation of inflammation-related genes involved in the cytokine activity pathway, the inflammatory response pathway, and the IL-17 signaling pathway in mouse thymocytes [42]. The NaVPA–NaDCA has a significant anti-inflammatory effect on specific sets of genes involved in inflammation and immune response pathways, including cytokine activity, chemokine-mediated signaling, neutrophil chemotaxis, and lymphocyte chemotaxis, in T lymphocytes from women with SARS-CoV-2 infection and pneumonia [44].

In the study, we discuss below the differences in the expression of *SLC12A2*, *SLC12A5*, *CDH1*, *CDH2*, *EZH2*, and *GFAP* in primary GBM IDH-wild-type female cells (GBM5-1F, GBM5-2F, and GBM5-3F), and the differences in the response of the tested cells to the effects of the treatment with NaVPA–NaDCA compared to the impact of the treatment with TMZ.

The cation and chloride cotransporters, the Na-K-2Cl cotransporter (NKCC1) and the K-Cl cotransporter (KCC2), are essential for the determination of intracellular Cl^- concentrations in neurons and GBM cells [67]. High-grade glioblastoma cells accumulate intracellular chloride ($[\text{Cl}^-]_i$) ~10 times more than the average of grade II glioma and normal cortical cells [68]. *SLC12A2*, the gene encoding NKCC1, is expressed in GBMs in primary patient biopsies and patient-derived xenografts. *SLC12A5*, the gene that encodes KCC2, which carries Cl^- out of the cell, is poorly expressed in GBMs [51]. Treatment with NaVPA–NaDCA or TMZ significantly reduced *SLC12A2* expression in GBM5-3F cells, which had significantly higher gene expression than GBM5-2F cells in the control group. Treatment with the NaVPA–NaDCA increased *SLC12A2* expression in both GBM5-1F and GBM5-2F cells, whereas treatment with TMZ did not affect gene expression in the TMZ-treated respective cells. It was reported that 50 μM TMZ significantly increased *SLC12A2* expression in glioblastoma PBT24 and SF8628 cell lines [69]. Researchers hypothesized that NKCC1 activity in TMZ-treated GBM cells is stimulated via cell volume regulatory kinases and a WNK-mediated signaling pathway, which is vital in protecting gliomas from loss of cell volume and $[\text{Cl}^-]_i$ in TMZ-treated cells [70,71], allowing GBM cells to rapidly adapt to the altered osmotic situation. Resistance to TMZ therapy is thought to be due to overexpression of the NKCC1 cotransporter, which enhances DNA repair mechanisms that protect against TMZ-induced apoptosis [72].

The expression of *SLC12A5* was significantly different in all the control cells tested. Specifically, cells exhibited GBM5-3F > GBM5-2F > GBM5-1F gene expression. NaVPA–NaDCA treatment significantly increased the relative expression of *SLC12A5* in GBM5-1F and GBM5-2F. In contrast, this treatment significantly reduced relative gene expression in GBM5-3F cells. TMZ treatment did not affect *SLC12A5* expression in all three cells tested. It was reported that TMZ treatment significantly increased *SLC12A5* expression in GBM PBT24 cells, while treatment of SF8628 cells did not affect gene expression [69]. However, the expression of *SLC12A2* should not only be considered unilaterally but also in terms of

changes in the expression of *SLC12A5*. Evaluation of both cotransporter genes together after NaVPA–NaDCA treatment reveals that exposure significantly increases *SLC12A2* expression in GBM5-1F and GBM5-2F cells, thereby increasing Cl^- influx, concomitant with increased Cl^- efflux, as observed when *SLC12A5* is activated in GBM5-1F and GBM5-2F cells, respectively, suggesting an interplay between their functions. In GBM5-3F cells, NaVPA–NaDCA inhibited the expression of *SLC12A2* (Cl^- influx) while significantly reducing the expression of *SLC12A5* (Cl^- efflux). KCC2 is a vital cancer marker related to tumor cell apoptosis. The reduction in the intracellular K^+ and Cl^- ion levels is related to the activation of caspases and triggers caspase cascade-related apoptosis mechanisms [73]. Furthermore, NKCC1 upregulation is associated with astrocyte swelling and a relatively high $[\text{Cl}^-]_i$ content [74], as well as a GABAA receptor-mediated excitatory response that facilitates seizure onset [75]. KCC2, conversely, is a neuron-specific Cl^- extruder that uses a K^+ gradient to maintain low $[\text{Cl}^-]_i$ levels and ensure the proper functioning of postsynaptic GABAA receptors. Low KCC2 expression and function are hallmarks of epileptic brain disorders. The effect of drugs that activate KCC2 function in GBM is important as a potential new therapeutic target for GBM [76].

The majority of GBM did not express *CDH1* [77]. It is a rare occurrence to encounter malignant gliomas with E-cadherin expression [78]. GBMs without epithelial phenotypes exhibit a substantial alteration of the cytoskeleton, which differs from the classical EMT of epithelial tumors, characterized by a shift in E-cadherin away from N-cadherin [79,80]. In our study, *CDH1* expression was detected in all control cells, with the highest expression levels observed in GBM-2F and GBM-3F. These cells exhibited significantly higher *CDH1* expression compared to GBM-1F. The VPA–NaDCA significantly increased *CDH1* expression in GBM5-1F only. TMZ only reduced *CDH1* expression in GBM5-1F cells. GBM5-1F and GBM5-2F exhibited similar *CDH2* expression, and their gene expression was higher than that of GBM5-3F cells. VPA–NaDCA treatment did not affect *CDH2* expression in the cells studied; however, TMZ treatment significantly reduced relative gene expression in GBM5-1F and GBM5-2F cells, but did not affect gene expression in GBM5-3F cells. The EMT process in gliomas may be exacerbated by enhanced *CDH2* expression, which is associated with unfavorable prognostic outcomes. *CDH2* was expressed in the majority of glioma cases, with no expression found in 10.3% of high-grade GBM [81].

The following research areas are the GBM markers *EZH2* and *GFAP* gene expression. The histone methyltransferase *EZH2* is often overexpressed in GBM, regulating gene transcription and promoting tumor genesis by inhibiting the function of tumor suppressor genes [82,83]. *EZH2* facilitates glioma proliferation, migration, and invasion [58]. The differences in *EZH2* expression between the control cells are significant in the tested cells: GBM53F > GBM2F or GBM5-1F. Treatment with NaVPA–NaDCA significantly increased relative *EZH2* expression in GBM5-1F and GBM5-2F and reduced GBM5-3F cell gene expression considerably. TMZ significantly increased gene relative expression in GBM5-2F cells only. The *EZH2*–*SLC12A5* axis in GBM lays a new foundation for the clinical translation of NaVPA–NaDCA treatment, offering new insights for precision GBM therapy. Our study demonstrates that NaVPA–NaDCA can upregulate *SLC12A5* expression, suggesting that this beneficial effect may counteract the effects of *EZH2* in GBM cells.

The following significant differences in *GFAP* expression were observed between the control: GBM5-2F < GBM5-1F and GBM5-3F. Treatment with NaVPA–NaDCA significantly upregulated *GFAP* expression in GBM5-2F, significantly downregulated it in GBM5-3F, and did not affect gene expression in GBM5-1F cells. TMZ treatment did not affect *GFAP* expression in the tested cells. The *Ezh2*^{CKO} mouse model demonstrates that the depletion of *Ezh2* from astrocytes significantly increases GFAP expression. Furthermore, experimental

studies indicate that the loss of EZH2 in astrocytes leads to disruption of the blood–brain barrier (BBB) [84].

A limitation of the study could be that the number of primary GBM cells studied was small and limited to women. Therefore, studies are needed on the impact of gender differences on treatment effects. Another limitation of the study was that it did not account for other mechanisms that influence protein levels or activity, thereby limiting the assessment of the mechanism to mRNA. However, the activity of the proteins studied is influenced by many mechanisms other than gene expression (mRNA). Regarding the lack of studies on protein levels, it is worth noting that the correlation between differentially expressed mRNA and mRNA/protein levels of the same gene is a topic of debate. Genome-wide correlation between mRNA and protein expression levels is notoriously poor; typically, 0–50% of mRNA levels correspond to protein expression, with a correlation between mRNA and protein expression levels of around 40% explanatory power across many studies. Correlations between differentially expressed mRNA profiles were low and even negative [85–88].

The studies clearly show that GBM tissue cells exhibit a polymorphic response to tested treatment, indicating the importance of assessing the effects of chemotherapeutic agents before treatment is administered to personalize treatment. NaVPA and NaDCA have been used for treatment for decades, have the potential to cross the BBB, and their safety profile and blood levels are well known, encouraging further testing for new GBM therapeutic indications. Our in vitro studies demonstrate that NaVPA–NaDCA treatment is superior to TMZ treatment in certain respects.

5. Conclusions

1. The combination of sodium valproate and sodium dichloroacetate, as well as temozolomide, had individual impacts in vitro on the *SLC12A2*, *SLC12A5*, *CDH1*, *CDH2*, *EZH*, and *GFAP* expressions in GBM5-1, GBM5-2F, and GBM5-3F primary cells of GBM wild-type tumors.
2. When assessing the changes in *SLC12A2* and *SLC12A5*, *CDH1* and *CDH2*, or *EZH2* and *GFAP* expressions after treatment with NaVPA–NaDCA or TMZ, it was found that NaVPA–NaDCA could have an advantage of antitumor activity, and that may be more effective than TMZ, but the effect is individual.
3. To determine the differences in the efficacy of NaVPA–NaDCA and TMZ, further preclinical studies are needed to investigate their effects on the expression and function of GBM pathogenesis-relevant proteins, as well as their effects on GBM carcinogenesis pathways in the research of individualized treatment.

6. Patents

The combination of VPA and NaDCA products is for the treatment of cancer (Official bulletin of the state patent bureau of the Republic of Lithuania, No. 6874, filling date 17 April 2020 [89]), A European patent application has been submitted (European patent application No. 21168796.7, filing date 16 April 2021 [90]).

Supplementary Materials: The following supporting information can be downloaded at: <https://www.mdpi.com/article/10.3390/pharmaceutics17091161/s1>, Table S1: *SLC12A2* and *GAPDH* expression data from female GBM patient cells in control and treated groups; Table S2: *SLC12A5* and *GAPDH* expression data from female GBM patient cells in the control and treated groups; Table S3: *CDH1* and *GAPDH* expression data from female GBM patient tumor cells in the control and treated groups; Table S4: *CDH2* and *GAPDH* expression data from female GBM patient tumor cells in the control and treated groups; Table S5: *EZH2* and *GAPDH* expression data from female GBM patient

tumor cells in the control and treated groups; Table S6: *GFAP* and *GAPDH* expression data from female GBM patient tumor cells in the control and treated groups.

Author Contributions: Conceptualization, L.A. and D.S.; Data curation, A.P., D.G. and L.A.; Formal analysis, D.G., D.S., L.A. and A.P.; Funding acquisition, L.A.; Investigation, D.G. and A.P.; Methodology, D.G.; A.P. and D.S.; Project administration, L.A.; Resources, L.A. and D.S.; Software, D.G.; Supervision and data analysis L.A. and D.S.; Validation, D.G. and A.P.; Visualization, D.G.; Writing—original draft, D.S., D.G., L.A., I.B. and A.V.; Writing—review and editing, D.G., L.A., A.P., I.B., A.V., J.Š. and D.S. All authors have read and agreed to the published version of the manuscript.

Funding: Project No. 02-014-K-0036 was funded under the European Union funds allocated for 2021–2027 under the activity “Promote innovation supply” of the progress measure No. 05-001-05-07 by Order No. 4-398 of the Minister of Economy and Innovation of the Republic of Lithuania of 19 July 2023; Registration No. 02-014-K-0036.

Institutional Review Board Statement: The Vilnius Regional Biomedical Research Ethics Committee (Lithuania) granted the authorization to conduct biomedical research on 11 November 2024, authorization No. 2024/11-1625-1077.

Informed Consent Statement: Written Informed consent was obtained from all patients involved in the study.

Data Availability Statement: The data presented in this study are available on request from the corresponding author.

Conflicts of Interest: Author Laimis Akramas was employed by the company Dca Farma, UAB. The remaining authors declare that the research was conducted in the absence of any commercial or financial relationships that could be construed as a potential conflict of interest.

Abbreviations

The following abbreviations are used in this manuscript:

BBB	blood–brain barrier
CDH1	E-cadherin
CDH2	N-cadherin
DCA	dichloroacetate
EZH2	enhancer of zest homolog 2
GABAA	γ-aminobutyric acid A receptor
GBM	glioblastoma
GFAP	glial fibrillary acidic protein
GPI	glycophosphatidylinositol
HDAC	histone deacetylase
IDH	isocitrate dehydrogenase
KCC2	K-Cl cotransporter (SLC12A5)
MGMT	methylated-DNA-protein-cysteine methyltransferase
NaDCA	sodium dichloroacetate
NaVPA	sodium valproate
NaVPA–NaDCA	sodium valproate and sodium dichloroacetate combination
NKCC1	Na-K-2Cl cotransporter (SLC12A2)
OS	overall survival
PDH	pyruvate dehydrogenase
PDK	pyruvate dehydrogenase kinase
PGK1	phosphoglycerate kinase 1
SLC5A8	sodium-coupled monocarboxylate transporter
TMZ	temozolomide
WNK1-OSR1-NKCC1	lysine-deficient protein kinase-1—oxidative stress responsive 1—NKCC1 pathway

References

- Ostrom, Q.T.; Cioffi, G.; Gittleman, H.; Patil, N.; Waite, K.; Kruchko, C.; Barnholtz-Sloan, J.S. CBTRUS Statistical Report: Primary Brain and Other Central Nervous System Tumors Diagnosed in the United States in 2012–2016. *Neuro-Oncology* **2019**, *21* (Suppl. 5), v1–v100. [\[CrossRef\]](#)
- Ostrom, Q.T.; Cioffi, G.; Waite, K.; Kruchko, C.; Barnholtz-Sloan, J.S. CBTRUS Statistical Report: Primary Brain and Other Central Nervous System Tumors Diagnosed in the United States in 2014–2018. *Neuro-Oncology* **2021**, *23*, iii1–iii105. [\[CrossRef\]](#)
- Ostrom, Q.T.; Rubin, J.B.; Lathia, J.D.; Berens, M.E.; Barnholtz-Sloan, J.S. Females have the survival advantage in glioblastoma. *Neuro-Oncology* **2018**, *20*, 576–577. [\[CrossRef\]](#) [\[PubMed\]](#)
- Grégoire, H.; Roncali, L.; Rousseau, A.; Chérel, M.; Delneste, Y.; Jeannin, P.; Hindré, F.; Garcion, E. Targeting Tumor Associated Macrophages to Overcome Conventional Treatment Resistance in Glioblastoma. *Front. Pharmacol.* **2020**, *11*, 368. [\[CrossRef\]](#) [\[PubMed\]](#)
- Parsons, D.W.; Jones, S.; Zhang, X.; Lin, J.C.-H.; Leary, R.J.; Angenendt, P.; Mankoo, P.; Carter, H.; Siu, I.-M.; Gallia, G.L.; et al. An integrated genomic analysis of human glioblastoma multiforme. *Science* **2008**, *321*, 1807–1812. [\[CrossRef\]](#) [\[PubMed\]](#)
- Brown, N.F.; Carter, T.J.; Ottaviani, D.; Mulholland, P. Harnessing the immune system in glioblastoma. *Br. J. Cancer* **2018**, *119*, 1171–1181. [\[CrossRef\]](#)
- Couturier, C.P.; Ayyadury, S.; Le, P.U.; Nadaf, J.; Monlong, J.; Riva, G.; Allache, R.; Baig, S.; Yan, X.; Bourgey, M.; et al. Single-cell RNA-seq reveals that glioblastoma recapitulates a normal neurodevelopmental hierarchy. *Nat. Commun.* **2020**, *11*, 3406. [\[CrossRef\]](#)
- Patel, A.P.; Tirosh, I.; Trombetta, J.J.; Shalek, A.K.; Gillespie, S.M.; Wakimoto, H.; Cahill, D.P.; Nahed, B.V.; Curry, W.T.; Martuza, R.L.; et al. Single-cell RNA-seq highlights intratumoral heterogeneity in primary glioblastoma. *Science* **2014**, *344*, 1396–1401. [\[CrossRef\]](#)
- Tan, A.C.; Ashley, D.M.; López, G.Y.; Malinzak, M.; Friedman, H.S.; Khasraw, M. Management of glioblastoma: State of the art and future directions. *CA Cancer J. Clin.* **2020**, *70*, 299–312. [\[CrossRef\]](#)
- Colopi, A.; Fuda, S.; Santi, S.; Onorato, A.; Cesarini, V.; Salvati, M.; Balistreri, C.R.; Dolci, S.; Guida, E. Impact of age and gender on glioblastoma onset, progression, and management. *Mech. Ageing Dev.* **2023**, *211*, 111801. [\[CrossRef\]](#)
- Stupp, R.; Hegi, M.E.; Gilbert, M.R.; Chakravarti, A. Chemoradiotherapy in malignant glioma: Standard of care and future directions. *J. Clin. Oncol.* **2007**, *25*, 4127–4136. [\[CrossRef\]](#) [\[PubMed\]](#)
- Stupp, R.; Mason, W.P.; van den Bent, M.J.; Weller, M.; Fisher, B.; Taphoorn, M.J.B.; Belanger, K.; Brandes, A.A.; Marosi, C.; Bogdahn, U.; et al. Radiotherapy plus concomitant and adjuvant temozolomide for glioblastoma. *N. Engl. J. Med.* **2005**, *352*, 987–996. [\[CrossRef\]](#)
- Stupp, R.; Brada, M.; van den Bent, M.J.; Tonn, J.-C.; Pentheroudakis, G. High-grade glioma: ESMO Guidelines Working Group High-grade glioma: ESMO Clinical Practice Guidelines for diagnosis, treatment and follow-up. *Ann. Oncol.* **2014**, *25* (Suppl. 3), iii93–iii101. [\[CrossRef\]](#) [\[PubMed\]](#)
- Krex, D.; Klink, B.; Hartmann, C.; von Deimling, A.; Pietsch, T.; Simon, M.; Sabel, M.; Steinbach, J.P.; Heese, O.; Reifenberger, G.; et al. Long-term survival with glioblastoma multiforme. *Brain* **2007**, *130*, 2596–2606. [\[CrossRef\]](#) [\[PubMed\]](#)
- Johnson, D.R.; O'Neill, B.P. Glioblastoma survival in the United States before and during the temozolomide era. *J. Neuro-Oncol.* **2012**, *107*, 359–364. [\[CrossRef\]](#)
- Zawlik, I.; Vaccarella, S.; Kita, D.; Mittelbronn, M.; Franceschi, S.; Ohgaki, H. Promoter methylation and polymorphisms of the MGMT gene in glioblastomas: A population-based study. *Neuroepidemiology* **2009**, *32*, 21–29. [\[CrossRef\]](#)
- Chen, R.; Smith-Cohn, M.; Cohen, A.L.; Colman, H. Glioma Subclassifications and Their Clinical Significance. *Neurotherapeutics* **2017**, *14*, 284–297. [\[CrossRef\]](#)
- Larrieu, C.M.; Storevik, S.; Guyon, J.; Zottola, A.C.P.; Bouchez, C.L.; Derieppe, M.-A.; Tan, T.Z.; Miletic, H.; Lorens, J.; Tronstad, K.J.; et al. Refining the Role of Pyruvate Dehydrogenase Kinases in Glioblastoma Development. *Cancers* **2022**, *14*, 3769. [\[CrossRef\]](#)
- Chinopoulos, C.; Seyfried, T.N. Mitochondrial Substrate-Level Phosphorylation as Energy Source for Glioblastoma: Review and Hypothesis. *ASN Neuro* **2018**, *10*, 1–27. [\[CrossRef\]](#)
- Shen, H.; Yu, M.; Tsoli, M.; Chang, C.; Joshi, S.; Liu, J.; Ryall, S.; Chornenkyy, Y.; Siddaway, R.; Hawkins, C.; et al. Targeting reduced mitochondrial DNA quantity as a therapeutic approach in pediatric high-grade gliomas. *Neuro-Oncology* **2020**, *22*, 139–151. [\[CrossRef\]](#)
- Sutendra, G.; Michelakis, E.D. Pyruvate dehydrogenase kinase as a novel therapeutic target in oncology. *Front. Oncol.* **2013**, *3*, 38. [\[CrossRef\]](#) [\[PubMed\]](#)
- Kankotia, S.; Stacpoole, P.W. Dichloroacetate and cancer: New home for an orphan drug? *Biochim. Biophys. Acta* **2014**, *1846*, 617–629. [\[CrossRef\]](#)
- Stacpoole, P.W.; Nagaraja, N.V.; Hutson, A.D. Efficacy of dichloroacetate as a lactate-lowering drug. *J. Clin. Pharmacol.* **2003**, *43*, 683–691. [\[CrossRef\]](#) [\[PubMed\]](#)

24. Stakišaitis, D.; Damanskienė, E.; Curkūnavičiūtė, R.; Juknevičienė, M.; Alonso, M.M.; Valančiūtė, A.; Ročka, S.; Balnytė, I. The Effectiveness of Dichloroacetate on Human Glioblastoma Xenograft Growth Depends on Na⁺ and Mg²⁺ Cations. *Dose-Response* **2021**, *19*, 1559325821990166. [\[CrossRef\]](#)
25. Zamzami, N.; Kroemer, G. The mitochondrion in apoptosis: How Pandora's box opens. *Nat. Rev. Mol. Cell Biol.* **2001**, *2*, 67–71. [\[CrossRef\]](#)
26. Santoro, F.; Botrugno, O.A.; Zuffo, R.D.; Pallavicini, I.; Matthews, G.M.; Cluse, L.; Barozzi, I.; Senese, S.; Fornasari, L.; Moretti, S.; et al. A dual role for Hdac1: Oncosuppressor in tumorigenesis, oncogene in tumor maintenance. *Blood* **2013**, *121*, 3459–3468. [\[CrossRef\]](#)
27. Stakišaitis, D.; Kapočius, L.; Valančiūtė, A.; Balnytė, I.; Tamošutis, T.; Vaitkevičius, A.; Sužiedėlis, K.; Urbonienė, D.; Tatarūnas, V.; Kilimaitė, E.; et al. SARS-CoV-2 Infection, Sex-Related Differences, and a Possible Personalized Treatment Approach with Valproic Acid: A Review. *Biomedicines* **2022**, *10*, 962. [\[CrossRef\]](#)
28. Zhang, Z.; Wang, Y.; Chen, J.; Tan, Q.; Xie, C.; Li, C.; Zhan, W.; Wang, M. Silencing of histone deacetylase 2 suppresses malignancy for proliferation, migration, and invasion of glioblastoma cells and enhances temozolomide sensitivity. *Cancer Chemother. Pharmacol.* **2016**, *78*, 1289–1296. [\[CrossRef\]](#)
29. Kwak, S.; Park, S.-H.; Kim, S.-H.; Sung, G.-J.; Song, J.-H.; Jeong, J.-H.; Kim, H.; Ha, C.H.; Kim, S.W.; Choi, K.-C. miR-3189-targeted GLUT3 repression by HDAC2 knockdown inhibits glioblastoma tumorigenesis through regulating glucose metabolism and proliferation. *J. Exp. Clin. Cancer Res.* **2022**, *41*, 87. [\[CrossRef\]](#)
30. Han, W.; Guan, W. Valproic Acid: A Promising Therapeutic Agent in Glioma Treatment. *Front. Oncol.* **2021**, *11*, 687362. [\[CrossRef\]](#) [\[PubMed\]](#)
31. Chang, C.-Y.; Li, J.-R.; Wu, C.-C.; Ou, Y.-C.; Chen, W.-Y.; Kuan, Y.-H.; Wang, W.-Y.; Chen, C.-J. Valproic acid sensitizes human glioma cells to gefitinib-induced autophagy. *IUBMB Life* **2015**, *67*, 869–879. [\[CrossRef\]](#)
32. Fang, E.; Wang, J.; Hong, M.; Zheng, L.; Tong, Q. Valproic acid suppresses Warburg effect and tumor progression in neuroblastoma. *Biochem. Biophys. Res. Commun.* **2019**, *508*, 9–16. [\[CrossRef\]](#)
33. Babu, E.; Ramachandran, S.; CoothanKandaswamy, V.; Elangovan, S.; Prasad, P.D.; Ganapathy, V.; Thangaraju, M. Role of SLC5A8, a plasma membrane transporter and a tumor suppressor, in the antitumor activity of dichloroacetate. *Oncogene* **2011**, *30*, 4026–4037. [\[CrossRef\]](#)
34. Veronezi, G.M.B.; Felisbino, M.B.; Gatti, M.S.V.; Mello, M.L.S.; Vidal, B.d.C. DNA Methylation Changes in Valproic Acid-Treated HeLa Cells as Assessed by Image Analysis, Immunofluorescence and Vibrational Microspectroscopy. *PLoS ONE* **2017**, *12*, e0170740. [\[CrossRef\]](#) [\[PubMed\]](#)
35. Singh, N.; Miner, A.; Hennis, L.; Mittal, S. Mechanisms of temozolomide resistance in glioblastoma—A comprehensive review. *Cancer Drug Resist.* **2021**, *4*, 17–43. [\[CrossRef\]](#)
36. Nóbrega, A.H.L.; Pimentel, R.S.; Prado, A.P.; Garcia, J.; Frozza, R.L.; Bernardi, A. Neuroinflammation in Glioblastoma: The Role of the Microenvironment in Tumour Progression. *Curr. Cancer Drug Targets* **2024**, *24*, 579–594. [\[CrossRef\]](#)
37. DeCordova, S.; Shastri, A.; Tsolaki, A.G.; Yasmin, H.; Klein, L.; Singh, S.K.; Kishore, U. Molecular Heterogeneity and Immunosuppressive Microenvironment in Glioblastoma. *Front. Immunol.* **2020**, *11*, 1402. [\[CrossRef\]](#) [\[PubMed\]](#)
38. Certo, M.; Tsai, C.-H.; Pucino, V.; Ho, P.-C.; Mauro, C. Lactate modulation of immune responses in inflammatory versus tumour microenvironments. *Nat. Rev. Immunol.* **2021**, *21*, 151–161. [\[CrossRef\]](#)
39. Abdel-Razek, E.A.-N.; Mahmoud, H.M.; Azouz, A.A. Management of ulcerative colitis by dichloroacetate: Impact on NFATC1/NLRP3/IL1B signaling based on bioinformatics analysis combined with in vivo experimental verification. *Inflammopharmacology* **2024**, *32*, 667–682. [\[CrossRef\]](#) [\[PubMed\]](#)
40. Amirzargar, M.A.; Yaghubi, F.; Hosseiniapanah, M.; Jafari, M.; Pourjafar, M.; Rezaeepoor, M.; Rezaei, H.; Roshanaei, G.; Hajilooi, M.; Solgi, G. Anti-inflammatory Effects of Valproic Acid in a Rat Model of Renal Ischemia/Reperfusion Injury: Alteration in Cytokine Profile. *Inflammation* **2017**, *40*, 1310–1318. [\[CrossRef\]](#)
41. Silva, M.F.B.; Aires, C.C.P.; Luis, P.B.M.; Rutter, J.P.N.; IJlst, L.; Duran, M.; Wanders, R.J.A.; de Almeida, I.T. Valproic acid metabolism and its effects on mitochondrial fatty acid oxidation: A review. *J. Inher. Metab. Dis.* **2008**, *31*, 205–216. [\[CrossRef\]](#)
42. Stakišaitis, D.; Kapočius, L.; Kilimaitė, E.; Gečys, D.; Šlekienė, L.; Balnytė, I.; Palubinskienė, J.; Lesauskaitė, V. Preclinical Study in Mouse Thymus and Thymocytes: Effects of Treatment with a Combination of Sodium Dichloroacetate and Sodium Valproate on Infectious Inflammation Pathways. *Pharmaceutics* **2023**, *15*, 2715. [\[CrossRef\]](#)
43. Skredėnienė, R.; Stakišaitis, D.; Valančiūtė, A.; Balnytė, I. In Vivo and In Vitro Experimental Study Comparing the Effect of a Combination of Sodium Dichloroacetate and Valproic Acid with That of Temozolomide on Adult Glioblastoma. *Int. J. Mol. Sci.* **2025**, *26*, 6784. [\[CrossRef\]](#) [\[PubMed\]](#)
44. Stakišaitis, D.; Kapočius, L.; Tatarūnas, V.; Gečys, D.; Mickienė, A.; Tamošutis, T.; Ugenskienė, R.; Vaitkevičius, A.; Balnytė, I.; Lesauskaitė, V. Effects of Combined Treatment with Sodium Dichloroacetate and Sodium Valproate on the Genes in Inflammation- and Immune-Related Pathways in T Lymphocytes from Patients with SARS-CoV-2 Infection with Pneumonia: Sex-Related Differences. *Pharmaceutics* **2024**, *16*, 409. [\[CrossRef\]](#) [\[PubMed\]](#)

45. Lee, S.Y. Temozolomide resistance in glioblastoma multiforme. *Genes Dis.* **2016**, *3*, 198–210. [[CrossRef](#)] [[PubMed](#)]
46. Arora, A.; Somasundaram, K. Glioblastoma vs temozolomide: Can the red queen race be won? *Cancer Biol. Ther.* **2019**, *20*, 1083–1090. [[CrossRef](#)]
47. Gaca-Tabaszewska, M.; Bogusiewicz, J.; Bojko, B. Metabolomic and Lipidomic Profiling of Gliomas—A New Direction in Personalized Therapies. *Cancers* **2022**, *14*, 5041. [[CrossRef](#)]
48. Medikonda, R.; Dunn, G.; Rahman, M.; Fecci, P.; Lim, M. A review of glioblastoma immunotherapy. *J. Neuro-Oncol.* **2021**, *151*, 41–53. [[CrossRef](#)]
49. Vander Heiden, M.G.; Cantley, L.C.; Thompson, C.B. Understanding the Warburg effect: The metabolic requirements of cell proliferation. *Science* **2009**, *324*, 1029–1033. [[CrossRef](#)]
50. Venkatesh, H.S.; Morishita, W.; Geraghty, A.C.; Silverbush, D.; Gillespie, S.M.; Arzt, M.; Tam, L.T.; Espenel, C.; Ponnuswami, A.; Ni, L.; et al. Electrical and synaptic integration of glioma into neural circuits. *Nature* **2019**, *573*, 539–545. [[CrossRef](#)]
51. Taylor, K.R.; Barron, T.; Hui, A.; Spitzer, A.; Yalçın, B.; Ivec, A.E.; Geraghty, A.C.; Hartmann, G.G.; Arzt, M.; Gillespie, S.M.; et al. Glioma synapses recruit mechanisms of adaptive plasticity. *Nature* **2023**, *623*, 366–374. [[CrossRef](#)]
52. Zhu, W.; Begum, G.; Pointer, K.; Clark, P.A.; Yang, S.-S.; Lin, S.-H.; Kahle, K.T.; Kuo, J.S.; Sun, D. WNK1-OSR1 kinase-mediated phospho-activation of Na⁺-K⁺-2Cl⁻ cotransporter facilitates glioma migration. *Mol. Cancer* **2014**, *13*, 31. [[CrossRef](#)]
53. Bortner, C.D.; Sifre, M.I.; Cidlowski, J.A. Cationic gradient reversal and cytoskeleton-independent volume regulatory pathways define an early stage of apoptosis. *J. Biol. Chem.* **2008**, *283*, 7219–7229. [[CrossRef](#)]
54. Okada, Y.; Maeno, E. Apoptosis, cell volume regulation and volume-regulatory chloride channels. *Comp. Biochem. Physiol. Part A Mol. Integr. Physiol.* **2001**, *130*, 377–383. [[CrossRef](#)]
55. Bortner, C.D.; Hughes, F.M.; Cidlowski, J.A. A primary role for K⁺ and Na⁺ efflux in the activation of apoptosis. *J. Biol. Chem.* **1997**, *272*, 32436–32442. [[CrossRef](#)] [[PubMed](#)]
56. Azevedo, F.V.P.d.V.; Zóia, M.A.P.; Lopes, D.S.; Gimenes, S.N.; Vecchi, L.; Alves, P.T.; Rodrigues, R.S.; Silva, A.C.A.; Yoneyama, K.A.G.; Goulart, L.R.; et al. Antitumor and antimetastatic effects of PLA2-BthTX-II from Bothrops jararacussu venom on human breast cancer cells. *Int. J. Biol. Macromol.* **2019**, *135*, 261–273. [[CrossRef](#)] [[PubMed](#)]
57. Fujii, R.; Imanishi, Y.; Shibata, K.; Sakai, N.; Sakamoto, K.; Shigetomi, S.; Habu, N.; Otsuka, K.; Sato, Y.; Watanabe, Y.; et al. Restoration of E-cadherin expression by selective Cox-2 inhibition and the clinical relevance of the epithelial-to-mesenchymal transition in head and neck squamous cell carcinoma. *J. Exp. Clin. Cancer Res.* **2014**, *33*, 40. [[CrossRef](#)] [[PubMed](#)]
58. Zhang, H.; Wang, Z.; Qiao, X.; Peng, N.; Wu, J.; Chen, Y.; Cheng, C. Unveiling the therapeutic potential of IHMT-337 in glioma treatment: Targeting the EZH2-SLC12A5 axis. *Mol. Med.* **2024**, *30*, 91. [[CrossRef](#)]
59. Mohammad, F.; Weissmann, S.; Leblanc, B.; Pandey, D.P.; Højfeldt, J.W.; Comet, I.; Zheng, C.; Johansen, J.V.; Rapin, N.; Porse, B.T.; et al. EZH2 is a potential therapeutic target for H3K27M-mutant pediatric gliomas. *Nat. Med.* **2017**, *23*, 483–492. [[CrossRef](#)]
60. Ma, S.; Wang, L.; Zhang, J.; Geng, L.; Yang, J. The role of transcriptional and epigenetic modifications in astroglioneogenesis. *PeerJ* **2024**, *12*, e18151. [[CrossRef](#)]
61. Ortiz, R.; Perazzoli, G.; Cabeza, L.; Jiménez-Luna, C.; Luque, R.; Prados, J.; Melguizo, C. Temozolomide: An Updated Overview of Resistance Mechanisms, Nanotechnology Advances and Clinical Applications. *Curr. Neuropharmacol.* **2021**, *19*, 513–537. [[CrossRef](#)] [[PubMed](#)]
62. Giunco, S.; Padovan, M.; Angelini, C.; Cavallin, F.; Cerretti, G.; Morello, M.; Caccese, M.; Rizzo, B.; d’Avella, D.; Della Puppa, A.; et al. Prognostic role and interaction of TERT promoter status, telomere length and MGMT promoter methylation in newly diagnosed IDH wild-type glioblastoma patients. *ESMO Open* **2023**, *8*, 101570. [[CrossRef](#)] [[PubMed](#)]
63. Miele, E.; Anghileri, E.; Calatuzzolo, C.; Lazzarini, E.; Patrizi, S.; Ciolfi, A.; Pedace, L.; Patanè, M.; Abballe, L.; Paterra, R.; et al. Clinicopathological and molecular landscape of 5-year IDH-wild-type glioblastoma survivors: A multicentric retrospective study. *Cancer Lett.* **2024**, *588*, 216711. [[CrossRef](#)] [[PubMed](#)]
64. Valdebenito, S.; Malik, S.; Luu, R.; Loudig, O.; Mitchell, M.; Okafo, G.; Bhat, K.; Prideaux, B.; Eugenin, E.A. Tunneling nanotubes, TNT, communicate glioblastoma with surrounding non-tumor astrocytes to adapt them to hypoxic and metabolic tumor conditions. *Sci. Rep.* **2021**, *11*, 14556. [[CrossRef](#)]
65. Cloughesy, T.F.; Cavenee, W.K.; Mischel, P.S. Glioblastoma: From molecular pathology to targeted treatment. *Annu. Rev. Pathol. Mech. Dis.* **2014**, *9*, 1–25. [[CrossRef](#)]
66. Prionisti, I.; Bühler, L.H.; Walker, P.R.; Jolivet, R.B. Harnessing Microglia and Macrophages for the Treatment of Glioblastoma. *Front. Pharmacol.* **2019**, *10*, 506. [[CrossRef](#)]
67. Barron, T.; Yalçın, B.; Su, M.; Byun, Y.G.; Gavish, A.; Shamardani, K.; Xu, H.; Ni, L.; Soni, N.; Mehta, V.; et al. GABAergic neuron-to-glioma synapses in diffuse midline gliomas. *Nature* **2025**, *639*, 1060–1068. [[CrossRef](#)]
68. Garzon-Muvdi, T.; Schiapparelli, P.; ap Rhys, C.; Guerrero-Cazares, H.; Smith, C.; Kim, D.-H.; Kone, L.; Farber, H.; Lee, D.Y.; An, S.S.; et al. Regulation of brain tumor dispersal by NKCC1 through a novel role in focal adhesion regulation. *PLoS Biol.* **2012**, *10*, e1001320. [[CrossRef](#)]

69. Damanskienė, E.; Balnytė, I.; Valančiūtė, A.; Alonso, M.M.; Preikšaitis, A.; Stakišaitis, D. The Different Temozolomide Effects on Tumorigenesis Mechanisms of Pediatric Glioblastoma PBT24 and SF8628 Cell Tumor in CAM Model and on Cells In Vitro. *Int. J. Mol. Sci.* **2022**, *23*, 2001. [\[CrossRef\]](#)
70. Gagnon, K.B.E.; England, R.; Delpire, E. Characterization of SPAK and OSR1, regulatory kinases of the Na-K-2Cl cotransporter. *Mol. Cell. Biol.* **2006**, *26*, 689–698. [\[CrossRef\]](#)
71. Dowd, B.F.X.; Forbush, B. PASK (proline-alanine-rich STE20-related kinase), a regulatory kinase of the Na-K-Cl cotransporter (NKCC1). *J. Biol. Chem.* **2003**, *278*, 27347–27353. [\[CrossRef\]](#) [\[PubMed\]](#)
72. Algharabil, J.; Kintner, D.B.; Wang, Q.; Begum, G.; Clark, P.A.; Yang, S.-S.; Lin, S.-H.; Kahle, K.T.; Kuo, J.S.; Sun, D. Inhibition of Na⁺-K⁺-2Cl[−] cotransporter isoform 1 accelerates temozolomide-mediated apoptosis in glioblastoma cancer cells. *Cell. Physiol. Biochem.* **2012**, *30*, 33–48. [\[CrossRef\]](#)
73. Bortner, C.D.; Cidlowski, J.A. Cell shrinkage and monovalent cation fluxes: Role in apoptosis. *Arch. Biochem. Biophys.* **2007**, *462*, 176–188. [\[CrossRef\]](#) [\[PubMed\]](#)
74. Chen, H.; Sun, D. The role of Na–K–Cl co-transporter in cerebral ischemia. *Neurol. Res.* **2005**, *27*, 208–286. [\[CrossRef\]](#)
75. Owens, D.F.; Kriegstein, A.R. Is there more to GABA than synaptic inhibition? *Nat. Rev. Neurosci.* **2002**, *3*, 715–727. [\[CrossRef\]](#)
76. Di Cristo, G.; Awad, P.N.; Hamidi, S.; Avoli, M. KCC2, epileptiform synchronization, and epileptic disorders. *Prog. Neurobiol.* **2018**, *162*, 1–16. [\[CrossRef\]](#)
77. Mikheeva, S.A.; Mikheev, A.M.; Petit, A.; Beyer, R.; Oxford, R.G.; Khorasani, L.; Maxwell, J.-P.; Glackin, C.A.; Wakimoto, H.; González-Herrero, I.; et al. TWIST1 promotes invasion through mesenchymal change in human glioblastoma. *Mol. Cancer* **2010**, *9*, 194. [\[CrossRef\]](#)
78. Lewis-Tuffin, L.J.; Rodriguez, F.; Giannini, C.; Scheithauer, B.; Necela, B.M.; Sarkaria, J.N.; Anastasiadis, P.Z. Misregulated E-Cadherin Expression Associated with an Aggressive Brain Tumor Phenotype. *PLoS ONE* **2010**, *5*, e13665. [\[CrossRef\]](#)
79. Kahlert, U.D.; Nikkhah, G.; Maciaczyk, J. Epithelial-to-mesenchymal(-like) transition as a relevant molecular event in malignant gliomas. *Cancer Lett.* **2013**, *331*, 131–138. [\[CrossRef\]](#)
80. Kahlert, U.D.; Maciaczyk, D.; Doostkam, S.; Orr, B.A.; Simons, B.; Bogiel, T.; Reithmeier, T.; Prinz, M.; Schubert, J.; Niedermann, G.; et al. Activation of canonical WNT/β-catenin signaling enhances in vitro motility of glioblastoma cells by activation of ZEB1 and other activators of epithelial-to-mesenchymal transition. *Cancer Lett.* **2012**, *325*, 42–53. [\[CrossRef\]](#) [\[PubMed\]](#)
81. Noh, M.-G.; Oh, S.-J.; Ahn, E.-J.; Kim, Y.-J.; Jung, T.-Y.; Jung, S.; Kim, K.-K.; Lee, J.-H.; Lee, K.-H.; Moon, K.-S. Prognostic significance of E-cadherin and N-cadherin expression in Gliomas. *BMC Cancer* **2017**, *17*, 583. [\[CrossRef\]](#) [\[PubMed\]](#)
82. Suvà, M.L.; Rheinbay, E.; Gillespie, S.M.; Patel, A.P.; Wakimoto, H.; Rabkin, S.D.; Riggi, N.; Chi, A.S.; Cahill, D.P.; Nahed, B.V.; et al. Reconstructing and reprogramming the tumor-propagating potential of glioblastoma stem-like cells. *Cell* **2014**, *157*, 580–594. [\[CrossRef\]](#) [\[PubMed\]](#)
83. Kim, E.; Kim, M.; Woo, D.-H.; Shin, Y.; Shin, J.; Chang, N.; Oh, Y.T.; Kim, H.; Rheey, J.; Nakano, I.; et al. Phosphorylation of EZH2 activates STAT3 signaling via STAT3 methylation and promotes tumorigenicity of glioblastoma stem-like cells. *Cancer Cell* **2013**, *23*, 839–852. [\[CrossRef\]](#) [\[PubMed\]](#)
84. Zhao, X.; Zhang, M.; Zou, W.; Li, C.; Zhang, S.; Lv, Y.; Su, L.; Ji, F.; Jiao, J.; Gao, Y. Ezh2 Regulates Early Astrocyte Morphogenesis and Influences the Coverage of Astrocytic Endfeet on the Vasculature. *Cell Prolif.* **2025**, *58*, e70015. [\[CrossRef\]](#)
85. de Sousa Abreu, R.; Penalva, L.O.; Marcotte, E.M.; Vogel, C. Global signatures of protein and mRNA expression levels. *Mol. Biosyst.* **2009**, *5*, 1512–1526. [\[CrossRef\]](#) [\[PubMed\]](#)
86. Vogel, C.; Marcotte, E.M. Insights into the regulation of protein abundance from proteomic and transcriptomic analyses. *Nat. Rev. Genet.* **2012**, *13*, 227–232. [\[CrossRef\]](#)
87. Koussounadis, A.; Langdon, S.P.; Um, I.H.; Harrison, D.J.; Smith, V.A. Relationship between differentially expressed mRNA and mRNA-protein correlations in a xenograft model system. *Sci. Rep.* **2015**, *5*, 10775. [\[CrossRef\]](#)
88. Buccitelli, C.; Selbach, M. mRNAs, proteins and the emerging principles of gene expression control. *Nat. Rev. Genet.* **2020**, *21*, 630–644. [\[CrossRef\]](#)
89. Official Bulletin of the State Patent Bureau of the Republic of Lithuania. Inventions Applications—2020 019–2021 526. Patents—6874–6876, 10 December 2021. Available online: <https://vpb.lrv.lt/uploads/vpb/documents/files/VPB-OB-Nr23-2021-12-10-1d.pdf> (accessed on 6 July 2025).
90. Donatas, S.; Angelija, V.; Ingrida, B.; Vaiva, L.; Milda, J.; Jurate, S.; Juozas, J.D. Derivative of Valproic Acid and Dichloroacetate Used for the Treatment of Cancer. European Patent Application No. 21168796.7, 20 October 2021. Available online: <https://register.epo.org/application?number=EP21168796> (accessed on 6 July 2025).

Disclaimer/Publisher’s Note: The statements, opinions and data contained in all publications are solely those of the individual author(s) and contributor(s) and not of MDPI and/or the editor(s). MDPI and/or the editor(s) disclaim responsibility for any injury to people or property resulting from any ideas, methods, instructions or products referred to in the content.